Finite Element Analysis for Underground Deep Excavation Behaviour in Phnom Penh City

Daro Roeun[1,*] Raksiri Sukkarak[2] and Suched Likitlersuang[1]

[1] *Centre of Excellence in Geotechnical and Geoenvironmental Engineering, Department of Civil Engineering, Faculty of Engineering, Chulalongkorn University 10330, THAILAND*

[2] *Department of Teacher Training in Civil Engineering, Faculty of Technical Education, King Mongkut's University of Technology North Bangkok 10800, THAILAND*

*Corresponding author; E-mail address: *6470185521@student.chula.ac.th*

Abstract

Underground space is urgently required to be used in economic imperative for landscape purposes in the Phnom Penh City of Cambodia due to the rapidly increasing economy and population over a few decades. Within the excavation work, lateral wall movement and ground surface settlement are critical concerns for engineers that could be affected the adjacent buildings, roads, etc. In this study, a deep excavation site located in Phnom Penh soft ground is selected to investigate. The 2D and 3D finite element analyses are utilised for predicting deep excavation behaviour, including lateral wall movement and ground surface settlement. The Mohr-Coulomb plasticity model was employed in deep excavation modelling. Empirical equations based on the maximum lateral wall movement and maximum ground surface settlement relationship are used to predict the wall movement and ground settlement profile. Finally, the results from finite element simulations, empirical analysis, and monitoring data are compared and discussed.

Keywords: Finite element analysis, Empirical analysis, Deep excavation, Phnom Penh

1. Introduction

In the last decade, Phnom Penh city has had a huge population increase, leading to a living space problem that forces people to use underground space for car parking, market, building, and transportation networks. The deep excavation in a downtown area is particularly challenging due to the limited space in the city. The excavation is a potential work to make space for saving underground spacing. Moreover, it has critical damage to adjacent buildings and infrastructure. It may result in wall movement and ground settlement caused by the changes in stress state during the excavation process. The retaining structure and supporting system are the most concern to make safety in constructing excavations. Many studies have analysed the effects of ground behaviour and supporting systems on deep excavations activity based on numerical model program [1-3].

PLAXIS commercial finite element software is helpful for numerical modelling to analyse ground behaviour [4]. Many research articles from various regions have been published and demonstrated an aspect of procedure modelling [5-7]. Two-dimensional (2D) and three-dimensional (3D) finite element (FE) analysis are commonly compared in finite element analysis due to the plan strain condition of 2D and the corner effect in 3D modelling. 2D FE analyses have been conducted by many practical engineer users most of the time due to the time-consuming and budget limitation for the company or other organizations. Although, the advantages of 2D analyses are fast convergence. On the other hand, 3D modelling allows users to model and analyse complex geometry and construction sequence of excavation, especially the corners effect of excavation [8-10].

The empirical analysis is a common approach to predict the wall movement and ground surface settlement based on correlating field monitoring data from the different field locations. That equation is used to estimate the excavation behaviour related to site condition instead of field monitoring data in case of unavailable field measurement [11-14]. The comparison of finite element analysis of PLAXIS 2D and 3D performance is focused on in this study. The plane strain and corner effect simulation will be demonstrated with a rectangular excavation shape (L/B = 1.17). The empirical equation based on previous experience data of research is used to predict wall

movement and ground surface settlement compared with simulation. The Mohr-Coulomb plasticity model is a constitutive soil model of numerical predictions to conduct on each 2D and 3D FE analysis.

2. Project background

In this work, the construction project site located on Kampuchea Krom Boulevard (128) in the downtown area of Phnom Penh city shows in Fig. 1. The Commercial development building project has 28-story with two underground basement floors. The excavation used a bottom-up construction method, which has a rectangular shape with 33 m in length and 28 m in width, and 8.5 m depth of excavation. The excavation uses contiguous piles wall (CPWs) with 0.6 m diameter (d) as retaining structures with 20 m length and H-type steel as strut system to support the structure as shown in Fig. 3.

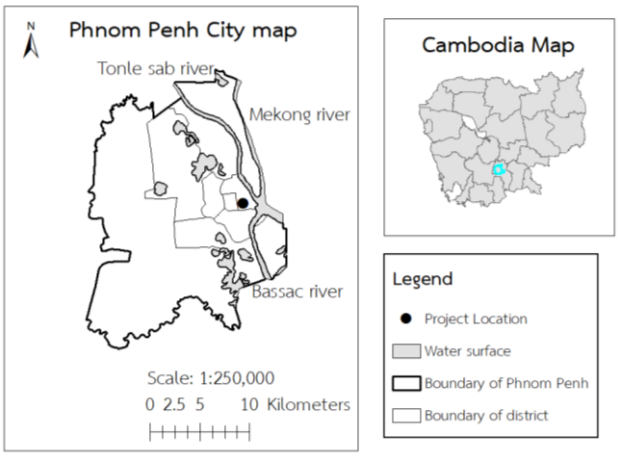

Fig. 1 The project location of research.

The maximum deep of excavations of project is 8.5 m below ground level. The excavation is in soft to medium clay layers. Fig. 3 shows the subsoil profile at the site consisting of an artificially filled, very loose state sand layer, approximately 3 m thick, followed by an 11 m thick, soft to medium stiff clay layer. The bellow is a stiff clay layer, with a thickness of 3.2 m, followed by a 2.3 m thick of a dense sand layer, and turn back very stiff clay and very dense sand with 3.5 m and 4 m, respectively. The last is a hard clay layer 3.5 m thick and followed by weathering rock layer at the bottom. The soft to medium stiff clay is a thick layer than others and where the excavation is located. The physical and mechanical properties of this layer had a bulk unit weight (γ_t) of 17.96 kN/m^3 – 18.71 kN/m^3, water content (w_n) of 27.8% - 47.7%, a void ratio (e) of 0.78 – 1.40, compression index (C_c) of 0.17 – 0.43, effective internal friction angle (ϕ') of 23° – 25.32°, and effective cohesion (c') of 16.7 kN/m^2 – 28.6 kN/m^2.

3. Numerical and empirical analyses of deep excavation

3.1 Soil constitutive model

The Mohr-Coulomb (MC) plasticity model is a well-known and simple model employed in deep excavation modelling, the most common constitutive law for describing soil behaviour. MC model is a combination of Hooke's law and Mohr-Coulomb's failure. The advantage of MC does not require many soil parameters for simulation, and those parameters can derive from conventional soil tests: Young modulus (E), Poisson's ratio (υ), friction angle (ϕ), cohesion (c), and dilatancy angle (ψ). In this paper, the constitutive model of Mohr-Coulomb developed in PLAXIS was directly used in the process of simulating the excavation.

The excavation of soil has been considered as the unloading behaviour of the ground. To consider the unloading problems, the unload-reload modus (E_{ur}^{ref}) recommend used instead of E_{50} for stiffness modulus in the MC model [15, 16].

Schanz, Vermeer [17] proposed E_{ur} should be converted to E_{ur}^{ref} for use as an input parameter in the hardening soil model.

$$E_{ur} = E_{ur}^{ref}\left(\frac{c.\cos\phi - \sigma_3^{'}\sin\phi}{c.\cos\phi + p_{ref}\sin\phi}\right)^m \quad (1)$$

$$E_{50} = E_{50}^{ref}\left(\frac{c.\cos\phi - \sigma_3^{'}\sin\phi}{c.\cos\phi + p_{ref}\sin\phi}\right)^m \quad (2)$$

Where E_{ur}^{ref} is equal to $3E_{50}^{ref}$, m is exponential power.

Architectural Institute of Japan (2001) [18] suggested the elastic modulus can apply to all soil types and effective elastic modulus (E) :

$$E' = 2800N \quad (3)$$

$$E' = E\frac{2(1+\upsilon')}{3} \quad (4)$$

Where υ' is effective poison's ratio, and E'(kPa) is effective elastic modulus.

In this study, secant modulus reference, E_{50}^{ref}, is conducted based on undrained consolidation triaxial testing as the main parameter for inputting the simulation. The calibration of the MC model and Consolidation Undrained Triaxial testing is presented in Fig. 2., which illustrates in stress-strain curve relationship. The testing involved applying different confining pressure: $\sigma_3'^{(1)} =$

25 kPa, $\sigma'^{(2)}_3 = 45$ kPa, $\sigma'^{(3)}_3 = 88$ kPa. The maximum deviator stress for each confining pressure was consistent between MC model and the Triaxial tests. However, the elastic of the MC model and the triaxial test depicted similar behaviors, yet the transaction between elastic-plastic behaviour is different. The soil testing exhibited the natural soil behavior, including the transaction between the elastic-plastic stage. However, the MC model displays the linear perfectly-plastic behavior, which generates soil stiffness is a higher value than the soil testing. The stiffness modulus of each confining pressure ($E^{(1)}_{50}$, $E^{(2)}_{50}$, $E^{(3)}_{50}$) from Fig. 2 are plotted in a linear line graph with the x-axis as $\ln((c.\cos\phi - \sigma'_3.\sin\phi)/(c.\cos\phi + p^{ref}.\sin\phi))$ and y-axis is $\ln E_{50}$. Then, using confining pressure σ'_3 = p^{ref} ($p^{ref} = 100$ kPa following PLAXIS default) to determine E^{ref}_{50}.

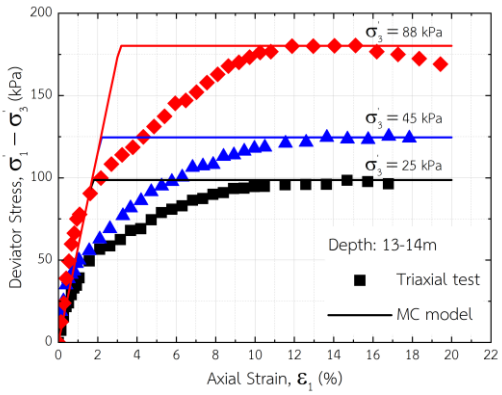

Fig. 2 Stress-strain calibration curve of MC with triaxial test.

3.2 Structural parameters

The retaining structure and supporting system in this excavation project selected CPWs and strut supporting systems. CPWs are performed continuously as bore piles in a row. Thus, the equivalent thickness of CPWs based on stiffness and wall area can be determined to be used in simulation [19]. For a circular area with a 0.6 m diameter of bore pile, the moment inertia of area can be determined as $I_{cir} = \pi D^4/64$. For a rectangular area, the moment inertia can be defined as $I_{rec} = b.h^3/12$. The length of the rectangular (b) is equal to the diameter of CPWs + spacing (s = 0.1 m). Thus, $h = 0.4777$ m is the equivalent wall thickness for input in Plaxis as plate element, which reduces 20.37% d. The main function of the strut support is to provide horizontal support to the wall. This study used two different struts to support level 1 and level 2 of excavation (S1: H300x300x10x15, S2: 400x400x13x21). Table 3 shows both input parameters of CPWs and struts for use in simulation. Other hand, the soil-interaction in finite element model is one of crucial parameter. The shear strength parameter (friction angle and cohesion) are reduced by the reduction factor (R_{inter}) close to the structure. The effects of R_{inter} is depended on disturbance of top soil layer and lower layer due excavation in rang 0.7-0.9 [1, 20]. The three top layers are selected 0.7 value and the rest are 0.9.

3.3 Numerical simulation

In this paper, the numerical simulation was conducted by using PLAXIS 2D and 3D. The borders of model, mesh density, and boundary conditions of both 2D and 3D models should influence the ground and wall movement behaviour.

Fig. 4 displays the boundary conditions, border conditions, and finite element mesh. The boundary conditions and dimensions of the simulation followed the suggestion by Bakker [21]. The border condition selected following the PLAXIS tutorial by fully fixing all boundaries except the top boundary where the deformation condition is displacement move freely. The mesh density in the nearby zone of excavation walls affects the accuracy of the result due to the majority expected of deformation in this area. To achieve quick convergence in the analyses, it is possible to have finer mesh in zones near the wall and use larger mesh sizes in areas farther from the excavation [22, 23].

3.4 Empirical analysis

The empirical expression of wall movement and ground surface settlement is a simple method developed to predict the displacement behaviour of deep excavation. Ou, Hsieh [12] and Hsieh and Ou [13] gave a relationship between maximum lateral displacement (δ_{hm}) and ground surface settlement (δ_{vm}) with the depth of excavation (H):

$$\delta_{hm} = 0.2\% - 0.5\%H \quad (5)$$

$$\delta_{vm} = 0.5 - 0.75\delta_{hm} \quad (6)$$

Table 1 Construction sequence of excavation.

Sequences	Construction activities
1	Cast-in-situ of CPWs, bore pile, and cap beam
2	Stage 1: Excavated to depth -2.0 m and installation strut1
3	Stage 2: Casing reinforced concrete 1.5 m thick at short length wall
4	Stage 2: Excavated to depth -5.0 m and installation strut1
5	Stage 3: Excavated to depth -8.5 m and installation strut2

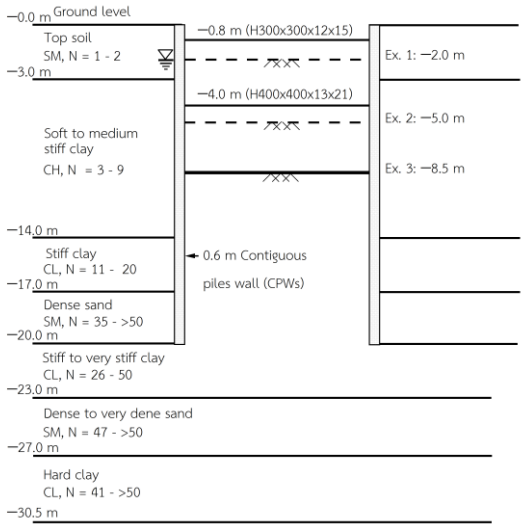

Fig. 3 Cross-section profile of excavation and subsoil condition of the project.

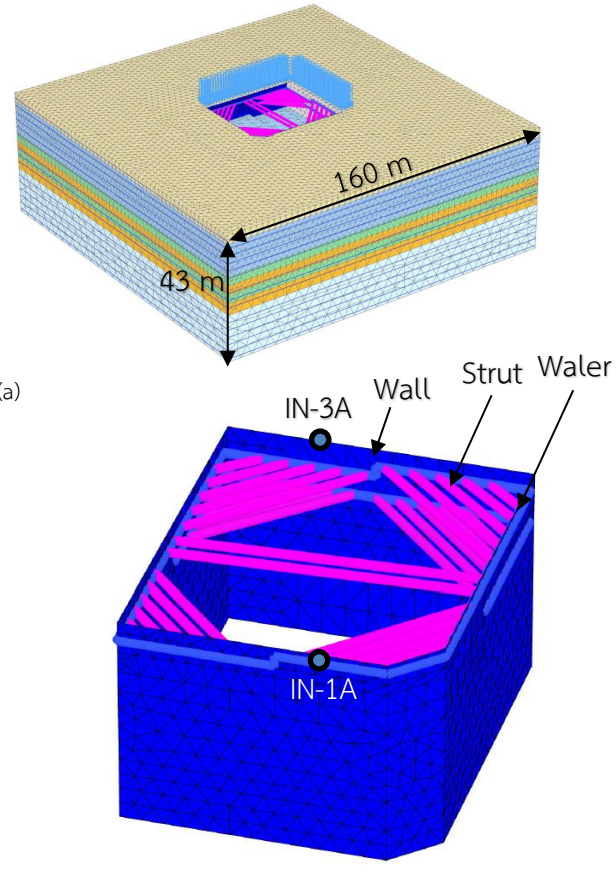

(a)

(b)

Fig. 4 FE model description: (a) model information; and (b) details of retaining structure and strut systems.

Based on statistically analysing using field measurement of deep excavation in Shanghai, Ding [24] and Zhang, Chen [11] proposed and simplified the general expression equation of the lateral displacement and ground surface settlement:

$$\delta_h(z) = A + B\exp\left[-\frac{(z-z_0)^2}{C^2}\right] \quad (7)$$

$$\delta_v(x/H) = \frac{(x/H)+0.75}{0.9}\exp\left\{-\frac{[x/H+0.75]^2}{4.5}\right\}\delta_{vm} \quad (8)$$

Where A, B, C and z_0 are coefficients determined by statistical from observation data in Table 2. $A = \delta_h(z)$ when $(z-z_0)^2$ is infinite with monitoring point at infinite distance from the point of z_0, $(A+B)$ is maximum lateral displacement of the wall, C is variation rate of δ_{hm} with z, z_0 is a depth of the maximum lateral displacement, $x/H \geq 0$; $x =$ distance between the monitoring point and the excavation.

Table 2 Mohr-Coulomb parameters

Soil	γ_b (kN/m^3)	N	c' (kPa)	ϕ' (°)	E (MPa)	ν'	ψ (°)	R_{inter}
SM	18.98	2	1	25	4.85	0.3	-	0.7
CH	18.23	6	16.7	23.92	18.00	0.35	-	0.7
CL	19.54	14	24.7	23.45	39.00	0.35	-	0.7
SM	20.96	47	1	34	114.09	0.3	4	0.9
CL	20.77	42	40.4	28.88	50.49	0.35	-	0.9
SM	21.19	50	1	34	121.38	0.3	4	0.9
CL	20.98	45	57.0	28.32	146.04	0.35	-	0.9

Table 3 Coefficient parameters for prediction [11].

Soil	Maximum	Minimum	Influence factor
A	0.019%H	0.009%H	Boundary condition
δ_{hm} = A + B	0.264%H	0.145%H	Stiffness of retaining
$z_0 = H\delta_{hm}$	0.660H	0.582H	Supporting system
C	0.631H	0.534H	Variation rate of δ_{hm}

4. Result and discussion

4.1 Lateral displacement

The wall movement behaviour of 2D and 3D models, empirical prediction, and field monitoring data at the final stage of excavation are depicted in Fig. 5. The Plain strain conditions of the 2D model result in the maximum value of wall movement. Therefore, to compare the 3D and 2D models, the maximum wall movement of the 3D model should be selected from the middle of the long-length wall. In a study by Goh, Zhang [25], the corner effects of 3D models were compared to plane strain conditions of 3D models using various ratios of L/B. The comparison showed that the magnitude of maximum wall deflection of 3D was a similar result or approaching the magnitude of the 2D model when L/B ratio was greater than or

equal to 2.2. Moreover, several publications have compared 2D and 3D modelling. Chheng and Likitlersuang [4] and Chen, Zhu [26] show good agreement results for project with L/B ratio greater than 2.2. However, this study has an ratio of L/B is 1.17, thus the maximum wall movement value between 2D and 3D model could not result in good agreement. Fig. 5 (a) and (b) show the comparison of 2D and 3D modelling results and empirical analysis. For the constitutive soil model, Mohr's coulomb model has been simulated with two different stiffness in simulation: MC1 ($E' = 3E_{50}^{ref}$) and MC2 ($E' = 1.5E_{50}^{ref}$) because the stiffness of MC1 is very stiff compared to the actual soil. For instance, Fig. 5 shows maximum wall movement value of MC1 is relatively small compared to MC2. For empirical prediction, based on Zhang, Chen [11] equation and the maximum wall deflection of Ou, Hsieh [12], the maximum value of the coefficient parameter in Table 3 and 0.005 times the maximum depth of excavation (8.5 x 0.005), δ_{hm} = 43 mm was applied to obtain the wall movement curve.

Fig. 5 (a) and (b) present a comparison of 2D and 3D model results of wall movement. The maximum wall movement value for MC1 and MC2 are 33.45 mm and 57.86 mm for 2D modelling, and 26.54 mm and 44.97 mm for 3D modelling, respectively. These results reveal that maximum wall movement of 2D models consistently demonstrate higher greater than 3D models by 6.92 mm (21%) and 12.89 mm (22%) for MC1 and MC2, respectively. Additionally, empirical observations indicate that the maximum wall movement and distribution curve is close to the 3D modelling of MC2 in Fig. 5 (b).

To compare the field monitoring data with 3D simulation, two inclinometer monitoring data (IN-1A and IN-3A) are available for comparison with 3D simulation. Fig. 5 (c) and (d) display the comparison of field monitoring data of the project with the 3D modelling of MC1 and MC2. The maximum wall movement of field monitoring data is 25.10 mm and 25.21 mm, while for 3D modelling of MC1 is 17.38 mm and 14.33 mm, and MC2 is 27.13 mm and 22.34 mm. Thus, the MC1 shows a wall performance of wall movement behaviour similar to the field monitoring data (IN-1A and IN-3A), but the magnitude of wall movement is comparatively smaller. On the other hand, MC2 exhibits a wall movement behaviour that does not fit well with field monitoring data; however, the magnitude of wall movement shows good agreement. The difference maximum of between field monitoring data and MC2 is 2.03 mm and 2.87 mm, respectively.

4.2 Ground surface settlement

According to Ou, Hsieh [12] and Ou, Chiou [23] concluded ground surface settlement behind the wall consists of a larger ground settlement occurring in a primary influence zone than a secondary influence zone. Additionally, Abbas, Yoon [27] defined the primary influence zone of the ground settlement behind the wall is 1.0 – 1.5 times of excavation depth (H) and larger at the corner side because of the combination of wall deflection at the corner.

Hsieh and Ou [13] suggested estimating the ground settlement based on maximum wall deflection relationship as mentioned in section 3.4 Eq. (4). The average value 0.625 of maximum wall deflection is selected. Fig. 6 compares 2D and 3D simulations with empirical prediction of ground settlement. The MC1 simulation shows a smaller value than MC2 simulation in both 2D and 3D. Fig. 6 (a) demonstrated that 3D ground settlement is smaller than 31.07% and 63.14% of 2D ground surface settlement compared to Fig. 6 (b). Fig. 6 (b) shows 3D ground settlement is smaller than 34% and 35.73% of 2D ground surface settlement compared to Fig. 6 (b). All the maximum ground surface settlements are in the primary influence zone with a range of 14.0 m – 27.25 m from the wall.

5. Conclusions

The finite element simulations of deep excavation in soft to medium clay in Phnom Penh city is exhibited in this study. The corner effect (L/B = 1.17) of 3D model shows wall movement is smaller than a plane strain of 2D model by 22%. Thus, the deep excavation project with an L/B ratio close to 1 value should be simulated with 3D modelling to avoid the overestimated wall movement. Otherwise, the ground surface settlement of 3D result is always smaller than 2D result due to the relationship between ground surface settlement and the lateral wall movement occurrence in primary influence zone. Moreover, 3D modelling can perform better in complex geometry and construction sequences of excavations.

Acknowledgement

The first author would like to acknowledge the Graduate School Programme of Chulalongkorn University for master's degree scholarship and Centre of Excellence in Geotechnical and Geoenvironmental Engineering for numerical software. Special thanks to Dr. Rithy Ouch and Mr. Sothoan Yoang for providing data for the analysis.

Table 4 Structural parameters for 2D and 3D.

Parameter	Structural Element	3D input						2D input	
		D (m)	A (m^2)	E (MPa)	n	I_2 (m^4)	I_3 (m^4)	EA (MN/m)	EI (MN/m2/m)
CBP	Plate	0.4777	-	$28x10^3$	0.15	-	-	$356x10^3$	254.40
Strut 1	Beam	-	0.01198	$200x10^3$	-	$0.2040x10^{-3}$	$0.0675x10^{-3}$	$2.396x10^3$	-
Strut 2	Beam	-	0.02190	$200x10^3$	-	$0.6662x10^{-3}$	$0.2242x10^{-3}$	$4.380x10^3$	-

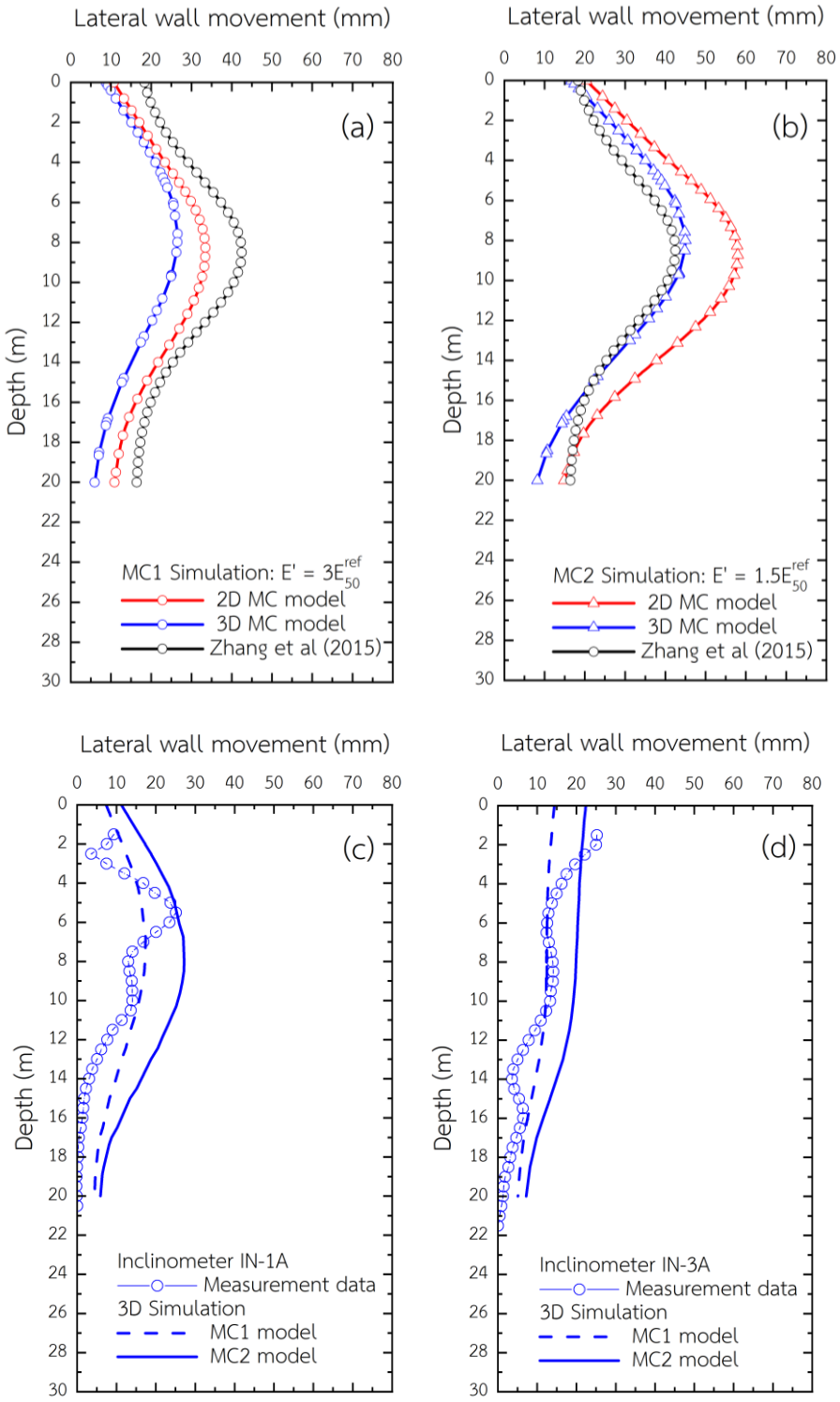

Fig. 5 Lateral wall movement comparison result of 2D, 3D, inclinometer, and empirical analysis: (a) Long length wall of MC1; (b) Long length wall of MC2; (c) Inclinometer IN-1A, MC1, and MC2; and (d) Inclinometer IN-3A, MC1, and MC2

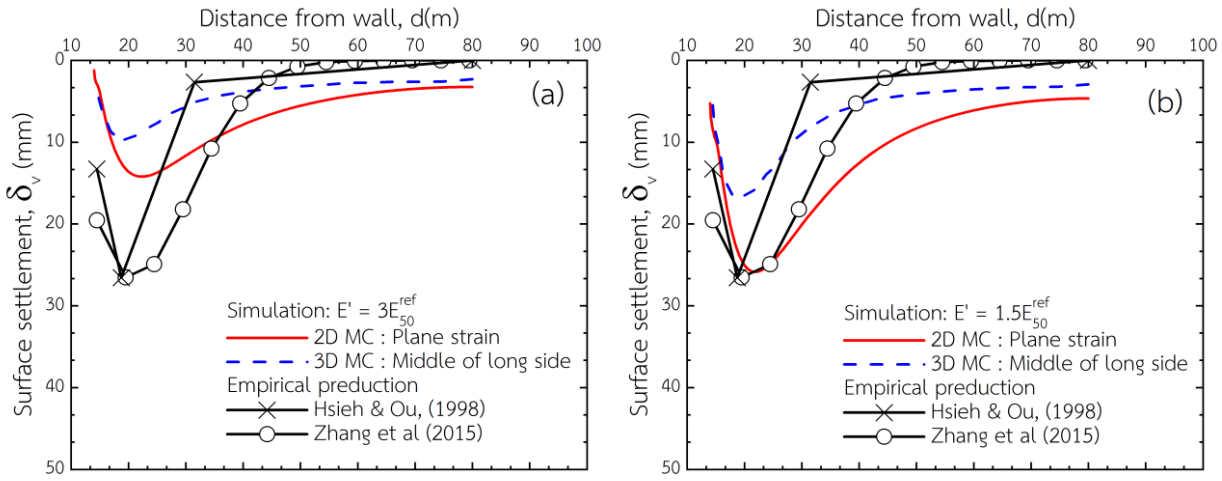

Fig. 6 Ground surface settlement comparison of 2D, 3D, and empirical analysis: (a) MC1, and (b) MC2

References

[1] Likitlersuang, S., C. Surarak, D. Wanatowski, E. Oh, and A. Balasubramaniam, *Finite element analysis of a deep excavation: A case study from the Bangkok MRT.* Soils and Foundations, 2013. **53**(5): p. 756-773.

[2] Likitlersuang, S., C. Chheng, and S. Keawsawasvong, *Structural modelling in finite element analysis of deep excavation.* Journal of GeoEngineering, 2019. **14**(3): p. 121-128.

[3] liu, B., W. Xu, D. Zhang, and Q. Zhang, *Deformation behaviors and control indexes of metro-station deep excavations based on case histories.* Tunnelling and Underground Space Technology, 2022. **122**: p. 104400.

[4] Chheng, C. and S. Likitlersuang, *Underground excavation behaviour in Bangkok using three-dimensional finite element method.* Computers and Geotechnics, 2018. **95**: p. 68-81.

[5] Hsiung, B.-C.B., K.-H. Yang, W. Aila, and C. Hung, *Three-dimensional effects of a deep excavation on wall deflections in loose to medium dense sands.* Computers and Geotechnics, 2016. **80**: p. 138-151.

[6] Jamsawang, P., S. Jamnam, P. Jongpradist, P. Tanseng, and S. Horpibulsuk, *Numerical analysis of lateral movements and strut forces in deep cement mixing walls with top-down construction in soft clay.* Computers and Geotechnics, 2017. **88**: p. 174-181.

[7] Lim, A., C.-Y. Ou, and P.-G. Hsieh, *A novel strut-free retaining wall system for deep excavation in soft clay: numerical study.* Acta Geotechnica, 2019. **15**(6): p. 1557-1576.

[8] Hsiung, B.-C.B., K.-H. Yang, W. Aila, and L. Ge, *Evaluation of the wall deflections of a deep excavation in Central Jakarta using three-dimensional modeling.* Tunnelling and Underground Space Technology, 2018. **72**: p. 84-96.

[9] Hsiung, B.-C.B., S. Likitlersuang, K.H. Phan, and P. Pisitsopon, *Impacts of the plane strain ratio on excavations in soft alluvium deposits.* Acta Geotechnica, 2020. **16**(6): p. 1923-1938.

[10] Schanz, T., *Zur modellierung des mechanischen verhaltens von reibungsmaterialen, habilitation.* Stuttgart Universität, Stuttgart, Germany, 1998.

[11] Zhang, H.-B., J.-J. Chen, X.-S. Zhao, J.-H. Wang, and H. Hu, *Displacement Performance and Simple Prediction for Deep Excavations Supported by Contiguous Bored Pile Walls in Soft Clay.* Journal of Aerospace Engineering, 2015. **28**(6).

[12] Ou, C.-Y., P.-G. Hsieh, and D.-C. Chiou, *Characteristics of ground surface settlement during excavation.* Canadian geotechnical journal, 1993. **30**(5): p. 758-767.

[13] Hsieh, P.-G. and C.-Y. Ou, *Shape of ground surface settlement profiles caused by excavation.* Canadian geotechnical journal, 1998. **35**(6): p. 1004-1017.

[14] Roboski, J. and R.J. Finno, *Distributions of ground movements parallel to deep excavations in clay.* Canadian Geotechnical Journal, 2006. **43**(1): p. 43-58.

[15] Lim, A. and C.-Y. Ou, *Stress paths in deep excavations under undrained conditions and its influence on deformation analysis.* Tunnelling and Underground Space Technology, 2017. **63**: p. 118-132.

[16] Brinkgreve, R., S. Kumarswamy, W. Swolfs, D. Waterman, A. Chesaru, and P. Bonnier, *PLAXIS 2016.* PLAXIS bv, the Netherlands, 2016.

[17] Schanz, T., P. Vermeer, and P. Bonnier, *The hardening soil model: formulation and verification, Beyond 2000 in Computational Geotechnics-10 Years of PLAXIS.* Balkema, Rotterdam, 1999: p. 1-16.

[18] Japan, A.I.o., *Recommendations of Design of Building Foundation*. 2001.

[19] Chai, J., J. Ni, W. Ding, Y. Qiao, and X. Lu, *Deep excavation in under-consolidated clayey deposit.* Underground Space, 2021. **6**(4): p. 455-468.

[20] Schweiger, H. *Design of deep excavations with FEM-Influence of constitutive model and comparison of EC7 design approaches*. in *Earth Retention Conference 3*. 2010.

[21] Bakker, K.J., *A 3D FE model for excavation analysis*, D. Delft University of Technology & Plaxis BV, The Netherlands, Editor. 2005, Proceeding of the 5th International Symposium TC28: INTERNATIONAL SOCIETY FOR SOIL MECHANICS AND GEOTECHNICAL ENGINEERING.

[22] Ahmadi, A. and M.M. Ahmadi, *Three-dimensional numerical analysis of corner effect of an excavation supported by ground anchors.* International Journal of Geotechnical Engineering, 2019. **16**(7): p. 903-915.

[23] Ou, C.-Y., D.-C. Chiou, and T.-S. Wu, *Three-Dimensional Finite Element Analysis of Deep Excavations.* Journal of Geotechnical Engineering, 1996. **122**(5): p. 337-345.

[24] Ding, Y., *Excavation-induced deformation and control in soft deposits*. 2009, Ph. D. thesis, Shanghai Jiao Tong Univ., Shanghai, China (in Chinese).

[25] Goh, A.T.C., F. Zhang, W. Zhang, Y. Zhang, and H. Liu, *A simple estimation model for 3D braced excavation wall deflection.* Computers and Geotechnics, 2017. **83**: p. 106-113.

[26] Chen, G., J. Zhu, M. Qiang, and W. Gong, *Three-dimensional site characterization with borehole data – A case study of Suzhou area.* Engineering Geology, 2018. **234**: p. 65-82.

[27] Abbas, Q., J. Yoon, and J. Lee, *Characterization of Wall Deflection and Ground Settlement for Irregular-Shaped Excavations with Changes in Corner Configuration.* International Journal of Geomechanics, 2023. **23**(1).